J Pathol Inform

Editor-in-Chief:
Anil V. Parwani , Pittsburgh, PA, USA
Liron Pantanowitz, Pittsburgh, PA, USA

OPEN ACCESS
HTML format

For entire Editorial Board visit : www.jpathinformatics.org/editorialboard.asp

Original Article

SIVQ-aided laser capture microdissection: A tool for high-throughput expression profiling

Jason Hipp[1], Jerome Cheng[1], Jeffrey C. Hanson[2], Wusheng Yan[2], Phil Taylor[3], Nan Hu[2], Jaime Rodriguez-Canales[2], Jennifer Hipp[2], Michael A. Tangrea[2], Michael R. Emmert-Buck[2], Ulysses J. Balis[1], and the Inflammation and the Host Response, Large-Scale Collaborative Research Program[4]

[1]Department of Pathology, University of Michigan School of Medicine, Division of Pathology Informatics, M4233 Med Sci I, 1301 Catherine, Ann Arbor, MI 48109-0602, [2]National Institutes of Health, National Cancer Institute, Laboratory of Pathology, Center for Cancer Research, Advanced Technology Center, Room 109, 8717 Grovemont Circle, Gaithersburg, MD 20877, [3]Division of Cancer Epidemiology and Genetics, Executive Plaza South, Room 7006, Rockville, MD 20892, USA, [4]Inflammation and the Host Response to Injury, Large Scale Collaborative Research Program is comprised of:
Lily Altstein, Ph.D., Henry V. Baker, Ph.D., Ulysses G.J. Balis, M.D., Paul E. Bankey, M.D., Ph.D., Timothy R. Billiar, M.D., Bernard H. Brownstein, Ph.D., Steven E. Calvano, Ph.D., David G. Camp II, Ph.D., J. Perren Cobb, M.D., Joseph Cuschieri, M.D., Ronald W. Davis, Ph.D., Asit K. De, Ph.D., Celeste C. Finnerty, Ph.D., Richard L. Gamelli, M.D., Nicole S. Gibran, M.D., Brian G. Harbrecht, M.D., Douglas L. Hayden, M.A., Laura Hennessy, R.N., David N. Herndon, M.D., Shari E. Honari, R.N., Marc G. Jeschke, M.D., Ph.D., Jeffrey L. Johnson, M.D., Matthew B. Klein, M.D., Stephen F. Lowry, M.D., Ronald V. Maier, M.D., Philip H. Mason, Ph.D., Grace P. McDonald-Smith, M.Ed., Bruce A. McKinley, Ph.D., Carol L. Miller-Graziano, Ph.D., Michael N. Mindrinos, Ph.D., Joseph P. Minei, M.D., Lyle L. Moldawer, Ph.D., Ernest E. Moore, M.D., Frederick A. Moore, M.D., Avery B. Nathens, M.D., Ph.D., M.P.H., Grant E. O'Keefe, M.D., M.P.H., Laurence G. Rahme, Ph.D., Daniel G. Remick, M.D., David A. Schoenfeld, Ph.D., Michael B. Shapiro, M.D., Richard D. Smith, Ph.D., Jason Sperry, M.D., John D. Storey, Ph.D., Robert Tibshirani, Ph.D., Ronald G. Tompkins, M.D., Sc.D., Mehmet Toner, Ph.D., H. Shaw Warren, M.D., Michael A. West, M.D., PhD., Bram Wispelwey, M.S., Wenzhong Xiao, Ph.D., Wing H. Wong, Ph.D.

E-mail: *Ulysses J. Balis - ulysses@umich.edu
*Corresponding author

Received: 26 January 11 Accepted: 22 February 11 Published: 31 March 11
DOI: 10.4103/2153-3539.78500 *J Pathol Inform* 2011, 2:19
This article is available from: http://www.jpathinformatics.org/content/2/1/19

This article may be cited as:
Hipp J, Cheng J, Hanson JC, Yan W, Taylor P, Hu N, Rodriguez-Canales J, Hipp J, Tangrea MA, Emmert-Buck MR, Balis U. SIVQ-aided laser capture microdissection: A tool for high-throughput expression profiling. J Pathol Inform 2011;2:19
Available FREE in open access from: http://www.jpathinformatics.org/text.asp? 2011/2/1/19/78500

Abstract

Introduction: Laser capture microdissection (LCM) facilitates procurement of defined cell populations for study in the context of histopathology. The morphologic assessment step in the LCM procedure is time consuming and tedious, thus restricting the utility of the technology for large applications. **Results:** Here, we describe the use of Spatially Invariant Vector Quantization (SIVQ) for histological analysis within LCM. Using SIVQ, we selected vectors as morphologic predicates that were representative of normal epithelial or cancer cells and then searched for phenotypically similar cells across entire tissue sections. The selected cells were subsequently auto-microdissected and the recovered RNA was analyzed by expression microarray. Gene expression profiles from SIVQ–LCM and standard LCM-derived samples demonstrated highly congruous signatures, confirming the equivalence of the differing microdissection methods. **Conclusion:** SIVQ–LCM improves the work-flow of microdissection in two significant ways. First, the process is transformative in that it shifts the pathologist's role from technical execution of the entire microdissection to a limited-contact supervisory role, enabling large-scale extraction of tissue by expediting subsequent semi-autonomous identification of target cell populations. Second, this work-flow model provides an opportunity to systematically identify highly constrained cell populations and morphologically consistent regions within tissue sections. Integrating SIVQ with LCM in a single environment provides advanced capabilities for efficient and high-throughput histological-based molecular studies.

Key words: Laser capture microdissection, microarray, Spatially Invariant Vector Quantization

INTRODUCTION

Laser capture microdissection (LCM) was developed as a tool for the isolation of specific cell populations from complex tissue specimens under microscopic visualization.[1] Since its invention in 1996, the technology has evolved significantly and there are now several different commercially available microdissection platforms. The incorporation of semi-automated features such as motorized microdissection stage actuation and improved software capabilities has further advanced the process. Laser microdissection technology is widely employed by laboratories for the molecular analysis of tissues, with nearly 3000 peer-reviewed studies now being available in the literature.[2,3] There is increasing scientific evidence demonstrating the necessity of upfront malignant cell enrichment techniques for specific molecular profiles as being especially desirable for clinical trials that require accurate, disease cell-specific molecular measurements.[4-7]

Laser dissection, despite its advances, is still a relatively tedious procedure, with it requiring visual microscopic identification of each target cell population by a trained investigator. The time consumed by the cell-by-cell selection process is often rate-limiting when many cells and/or many samples require dissection. Espina *et al*. described the major limitation of LCM as the need to identify cells of interest based on morphologic characteristics.[2] A lengthy dissection interval can compromise the molecular integrity of the recovered biomolecules. One approach to increase dissection throughput is to utilize molecular probes to facilitate the process. Expression microdissection (xMD) is such an example where an antibody is used for cell targeting in place of an investigator.[8,9] A recently described method for image segmentation and feature extraction of histopathological images, known as Spatially Invariant Vector Quantization (SIVQ),[10] differs fundamentally from the majority of established image analysis algorithms. SIVQ exhibits significant freedom from context-specific performance restrictions and at the same time provides for a rapid and interactive discovery work-flow model. Its potential use as a tool for computational-assisted LCM is further enhanced by its inherently simple user interface and associated modest training requirements. These attributes comprise an ideal turnkey platform for general histological feature selection and pattern recognition tasks, which can be carried out equally well by non–microscopy-trained personnel and subject matter experts (SMEs) alike.

Proposed SIVQ-based Work-flow Model

The SIVQ software discovery engine utilized in this study is compatible with the majority of commonly encountered digital image file formats (e.g. bmp, jpg, tiff, and most WSI formats). Initially, one (or a small number of) distinct predicate image candidate feature is identified by the user. This histological feature is utilized to perform an exhaustive search of the entire surface area of digital whole slide imagery (WSI), resulting in the generation of a statistical probability heatmap of morphologically similar regions. The unique aspects of SIVQ, as a pattern matching algorithm, can be further reviewed in Hipp and Cheng *et al.*[10]

In the present study, our goals were to incorporate the basic SIVQ method into the integral work-flow of a commercially available laser microdissection instrument, producing a decrease in human contact time with the machine, and to enable non-domain experts (i.e. non–microscopy-trained personnel) to perform microdissection on an equal footing with SMEs. The final goal was to establish a high-throughput tissue procurement pipeline for the identification of specific morphologic cell types in large preparative quantities, which could then facilitate high-throughput expression studies.

MATERIALS AND METHODS

Spatially Invariant Vector Quantization

The use of SIVQ image analysis has been previously described elsewhere by Hipp and Cheng *et al.*[10] An additional feature was added to automatically re-embed the LCM positional coordinates from the pre-processed image onto the post-processed image.

Tissue Specimens and Slide Preparation

To evaluate the efficiency of SIVQ for histological analysis and LCM, we tested four different tissue types.

Esophagus

Two snap-frozen human esophageal specimens with squamous cell carcinoma and normal squamous cell epithelium were studied. Both cases were obtained from subjects residing in the Taihang mountain region of north central China as part of a study that was approved by the Institutional Review Boards of the collaborating institutions: Shanxi Cancer Hospital and Institute, Taiyuan, Shanxi Province, China, and the National Cancer Institute, Bethesda, MD, USA. From each of the esophageal cases, normal and tumor epithelial samples were processed in separate tissue blocks, embedded in optimal cutting temperature compound (OCT), and 8-μm thick sections were cut in a Leica Cryostat CM1850-UV (Leica Microsystems Nussloch GmbH, Nußloch Germany)

Dog prostate

A canine normal prostate specimen, formalin fixed and paraffin embedded, was obtained following the National Institutes of Health regulations and guides for the care and use of laboratory animals.

Human prostate tissue

Tissue from a human radical prostatectomy specimen

with cancer was ethanol fixed and paraffin embedded. Histological sections were mounted on both charged and uncharged glass slides. The prostate specimen was obtained from an IRB-approved study at the National Cancer Institute, Bethesda, MD, and the sample and its associated identifying demographic was anonymized, prior to use.

Human breast tissue

A formalin-fixed, paraffin-embedded (FFPE) human breast cancer specimen containing a high-grade ductal cell adenocarcinoma was obtained from the Cooperative Human Tissue Network at the National Cancer Institute following established procedures.

Histological Slide Preparation

From each case, samples were microdissected using a standard LCM procedure, and established molecular extraction protocols were used to process the recovered biomolecules.[11] Parallel tissue section recuts were dissected using the SIVQ–LCM procedure. For traditional LCM, tissue sections from each block were mounted on uncharged glass slides and stained with hematoxylin–eosin (HandE) as previously described.[11] For SIVQ–LCM, tissue sections were mounted on either uncharged glass slides or polyethylene naphthalate (PEN) membrane slides (Applied Biosystems – Life Technologies, Carlsbad, CA, USA; Catalog number LCM0522), which are specialized slides for laser microdissection. PEN membrane slides require fewer infrared shots, thus enabling more efficient removal of the tissue from the slide. The optimal staining procedures that were compatible with both methods were evaluated. The HandE protocol[11] was compared against molecular grade Toluidine blue staining (Applied Biosystems, HistoGene Staining Solution, KIT04054), a fast, one-step ortho and metachromatic histochemical stain compatible with LCM and subsequent molecular analysis.

Traditional Laser Capture Microdissection

HandE stained slides of normal and tumor epithelium were laser capture microdissected using a PixCell II microscope (Arcturus Engineering, Carlsbad, CA, USA), as previously described.[11]

SIVQ–LCM Procedure

For the SIVQ–LCM tests, an Arcturus XT™ Microdissection System (Applied Biosystems) was utilized. The instrument was equipped with both near-infrared and UV lasers, allowing for both capture- and cutting-based microdissection. Additionally, the microdissection system was implemented with an AutoScan™ analysis software module that allows the user to image the tissue section on the stage, draw areas to be dissected, and then microdissect those regions in a semi-automated fashion. For SIVQ–LCM, we added an additional step to the work-flow. After the tissue section was imaged on the stage, we exported the image with its positional coordinates into SIVQ. Vectors were chosen and the image was analyzed. The image with the selected features after the analysis (i.e. a "painted" image) was converted back into a jpeg file and the positional coordinates were re-embedded. The image was subsequently re-imported into AutoScan to train the software to recognize the painted areas as a region of interest (ROI) and create a microdissection map. An LCM cap was placed onto the slide and near-infrared laser pulses were automatically fired within the mapped areas, causing the tissue to adhere to the cap. The UV laser then cut the target tissue borders, the cap was removed, and both the tissue on the cap and the remaining tissue were imaged. The time from the initial imaging step to dissection was under 30 minutes.

RNA Extraction and Microarray Analysis

Global transcript levels in the esophageal cases were analyzed using expression microarrays. The samples included the basal layer from normal epithelium and matching tumor from each case. RNA was isolated using the PicoPure RNA extraction kit (Applied Biosystems, catalog number KIT0204) as previously described.[11] RNA samples were amplified and hybridized on an Affymetrix U133A 2.0 GeneChip according to standard protocols. The data set was analyzed and then compared to previously published data in which the basal layer of normal epithelium and esophageal cancers were microdissected using traditional LCM. The samples were then imported and analyzed with BRB-Array Tools 4.0. The gene lists were filtered to identify the most highly and differentially expressed genes (less than 50% of expression values had at least twofold change, thus 70% of results were filtered out) and the data were clustered using centered correlation and average linkage.

RESULTS

We modified the Arcturus XT LCM protocol by adding an additional SIVQ image analysis step. In order to best utilize SIVQ, we first explored different techniques to improve the tissue image quality and subsequent microdissection process using either standard charged glass slides or specialized membrane-dissection glass slides. The effects of tissue processing (snap-frozen versus formalin-fixed, paraffin-embedded), staining, and digital enhancement of the images were evaluated.

Tissue and Slide Processing

With respect to overall tissue processing, we observed that optimal image quality with the specialized membrane glass slides employed for LCM (as described in the Materials and Methods Section) was obtained when using an automated HandE staining system. Also, as expected, the histological detail of frozen tissue sections was generally inferior to FFPE tissue due to freezing

artifact; however, given that cryostat sections produce high-quality DNA and RNA and are thus necessary for some molecular studies, we further adapted SIVQ–LCM for frozen sections using modifications in the protocol.

For the initial images taken on the Arcturus XT instrument, we started with ethanol-fixed, paraffin-embedded, HandE-stained human prostate tissue [Figure 1a, c] and noted that the quality of the image was poor due to the absence of a refractive index-matching cover slip (which cannot be used for LCM due to its interference with the capture process). We could improve the image quality slightly by adding 50 μl of ethanol on top of the tissue, enhancing the refractive index matching to that of a cover slip [Figure 1b], but optimal images were obtained by coating the tissue section with 30 μl of xylene [Figure 1d]. The use of xylene was advantageous since it is normally used as the final step in the slide preparation, prior to microdissection. Moreover, xylene treatment does not cause RNA degradation in the tissue section and evaporates quickly after imaging, thus alleviating the need for a removal step, which could have the effect of slowing microdissection work-flow. The image quality was then further improved by use of a digital image enhancement process (namely, the "Auto Correct" function of Microsoft Office Picture Manager, which is a contrast/white balance Histogram Equalization-type operator). The use of this tool significantly increased the sharpness and contrast of images, as observed in Figure 1e and f.

As expected, the image quality of the modified HandE protocol on frozen sections was poor as compared to the prostate tissue described above [Figure 2a, b]. Esophageal epithelium and stroma were of similar color and there was "bleeding" of stromal staining into the epithelium and vice versa. In an attempt to overcome this problem, we stained the frozen tissue with either eosin or hematoxlyin alone, but this resulted in unsatisfactory staining, which exhibited nearly identical coloring of both the stromal and epithelial features [Figure 2c–e]. However, Toluidine blue metachromatic staining proved to be uncomplicated, rapid and highly effective in accomplishing differential labeling between stroma and epithelium, with no bleed-over between adjacent cells or structures. Consequently, we selected this method as the preferred staining protocol for all subsequent frozen tissue investigations [Figure 3].

SIVQ–LCM

After imaging of Toluidine blue stained esophageal slides on the XT instrument, the resultant "Auto Corrected"

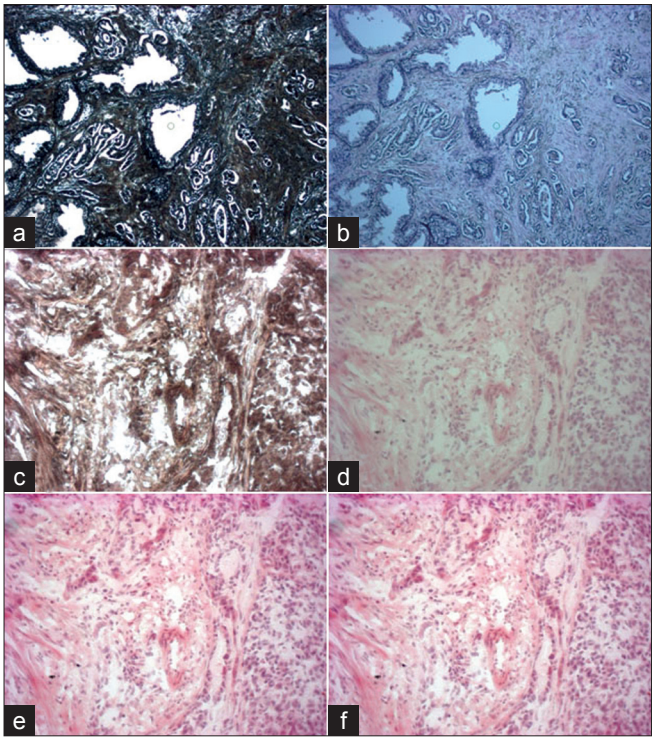

Figure 1: Hydration with different solvents to improve image quality. (a) A tissue section of ethanol-fixed, paraffin-embedded human prostate stained with HandE and imaged without a cover slip. (b) The corresponding field of view (FOV) of Figure 1a, but with 50 µl of ethanol. (c) A different field of Figure 1a without a cover slip. (d) The corresponding FOV of Figure 1c with 30 µl of xylene. (e) The corresponding FOV of Figure 1d that has been "Auto Corrected". (f) The same as Figure 1d, but which has been "Auto Corrected" a second time

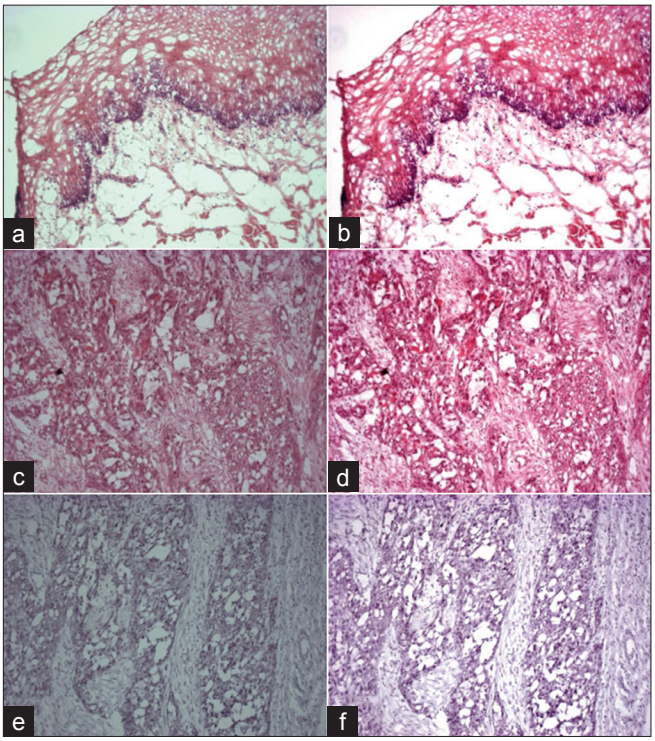

Figure 2: Exploration of staining methods. (a) Represents frozen human esophageal tissue stained with HandE and (b) is the same as Figure 2a but has been "Auto Corrected". (c) Represents frozen esophogeal squamous carcinoma stained with Eosin alone, and (d) is the same as Figure 2c but has been "Auto Corrected". (e) Represents frozen esophogeal squamous carcinoma stained with Hematoxalin alone and (f) is the same as Figure 2e but has been "Auto Corrected"

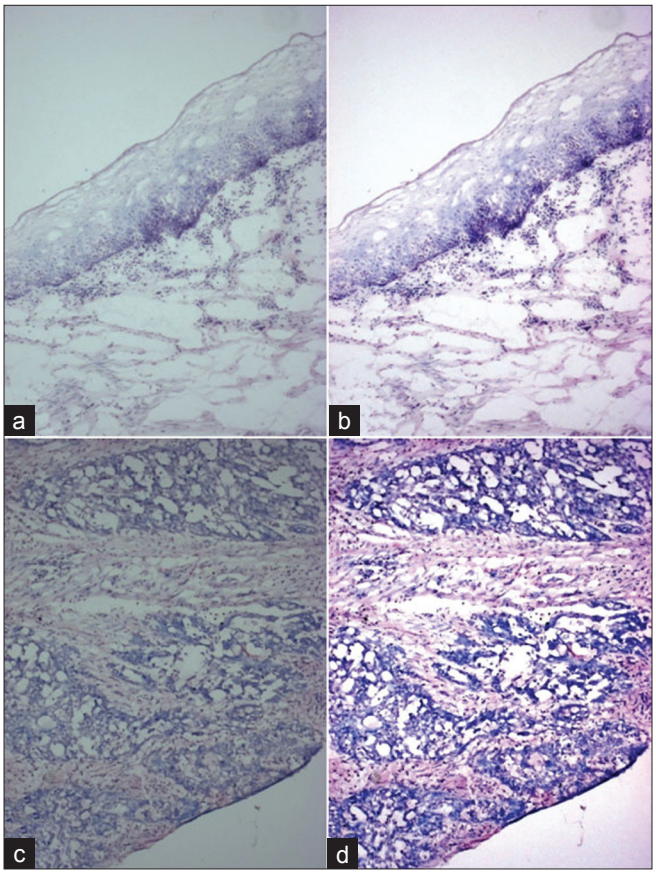

Figure 3: Frozen normal human esophagus and esophageal squamous cell carcinoma stained with Toluidine blue. (a) Frozen normal human esophageal tissue stained with Toluidine blue and (b) is the same field of view of Figure 3a that has been "Auto Corrected". (c) Frozen human esophageal squamous cell carcinoma stained with Toluidine blue and (d) is Figure 3c that has been "Auto Corrected"

images were imported into the SIVQ application. Vectors were chosen to identify normal and tumor-containing epithelium, with this step typically requiring about 1 minute, using a standard dual-core 2 GHz Pentium processor (as available on the typical XT system). On average, an area equal to the size of one LCM cap (6 mm) took approximately 3 minutes to scan. However, we were subsequently able to decrease this time to ~30 seconds by analyzing one-quarter of the pixels (e.g. at one-eighth of the Nyquist sampling frequency spatial limit).

Figure 4 depicts the entire procedure of utilizing SIVQ–LCM to selectively procure the basal stem cell containing compartment of normal squamous esophageal epithelium. The vector analysis resulted in a painted image that was imported into the Arcturus XT AutoScan software after the positional coordinates in the original jpeg file were re-embedded. The SIVQ application was modified to remove the coordinates from the original image and re-embed them automatically when the thresholded image was saved. The AutoScan software

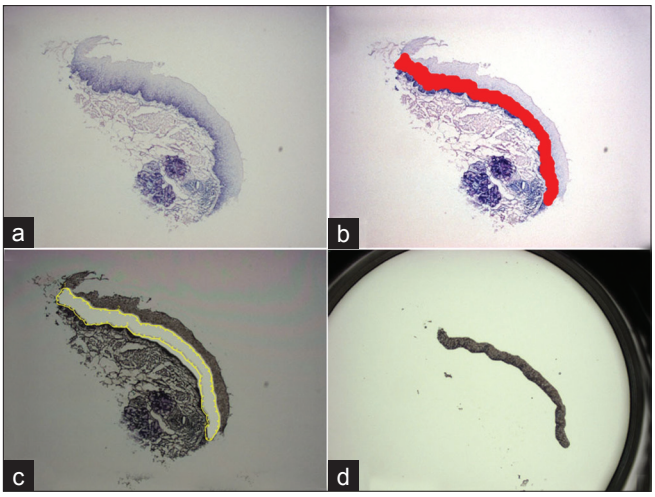

Figure 4: Frozen normal human esophageal tissue dissected for expression microarray analysis. (a) Frozen normal human esophageal tissue stained with Toluidine blue. A single vector was chosen to identify the normal epithelium with SIVQ (b). That area was microdissected and the remaining tissue is shown in (c). The cells that were used to isolate RNA and used for the microarrays are shown in (d)

of the XT microdissection instrument then highlighted such thresholded areas and auto-microdissected the target cells, with this process taking about 5 minutes to complete. The overall procedure was of less than 30 minutes in duration – an interval well within the dissection time frame that is recommended for mRNA-based analyses.

SIVQ–LCM → RNA Expression Microarrays

In order to compare and contrast data generated by SIVQ–LCM versus usual phenotype-based LCM, we performed expression microarray analysis on normal esophageal epithelium and matched the tumor using both dissection methods. For LCM, a standard dissection protocol was employed as described in a separate study.[11] For SIVQ–LCM, tissue sections were cut and placed onto membrane slides and subsequently stained with Toluidine blue. The tissue sections were then imaged on the Arcturus XT and "Auto Corrected" to improve the image quality. Finally, separate vectors for normal basal epithelium [Figure 4] and tumor areas [Figure 5] were selected. The resultant thresholded images were then re-imported into the Arcturus XT AutoScan software, allowing for specimens to be microdissected.

Total RNA from the normal and tumor samples were immediately isolated and analyzed on Affymetrix U133A 2.0 GeneChips. The resultant expression data were imported and analyzed using BRB-Array Tools 4.0 and then compared to previously published data for normal basal layer and tumor tissue dissected by standard LCM. The gene lists were filtered to identify the most highly and differentially expressed genes and the samples were clustered using centered correlation and average linkage. SIVQ–LCM normal and tumor samples clustered closely

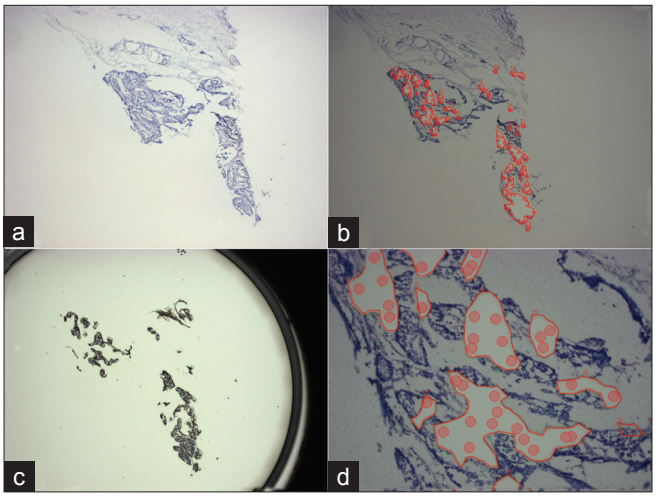

Figure 5: Frozen human esophageal squamous cell carcinoma dissected for expression microarray analysis. (a) Shows the cancer in dark blue and the stroma in light blue. A single vector was chosen to identify the cancer and the dissected cells and the remaining tissue are shown in (b). (c) The tissue was dissected and used for the microarrays. (d) A higher-power view of the remaining tissue, demonstrating a map of the tissue that was microdissected; the red circles within the microdissected areas correspond to the laser shots that were used to adhere the tissue to the cap

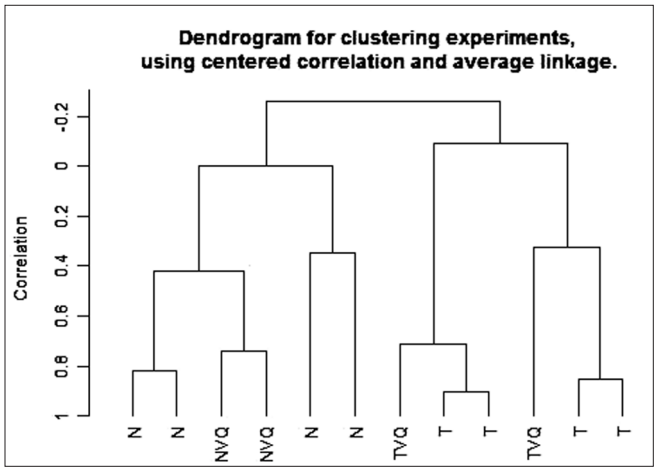

Figure 6: Dendrogram of the expression microarray data generated by standard LCM versus SIVQ–LCM. Samples labeled N correspond to normal esophageal tissue dissected by LCM. NVQ corresponds to normal esophageal tissue that was dissected by SIVQ–LCM. Samples labeled T correspond to esophageal squamous cell carcinoma tissue dissected by LCM. TVQ corresponds to esophageal squamous cell carcinoma dissected by SIVQ–LCM. The microarray data were filtered as follows: less than 50% of expression values having at least twofold change, 70% of data missing or filtered out. The dendrogram was created using a centered correlation and average linkage

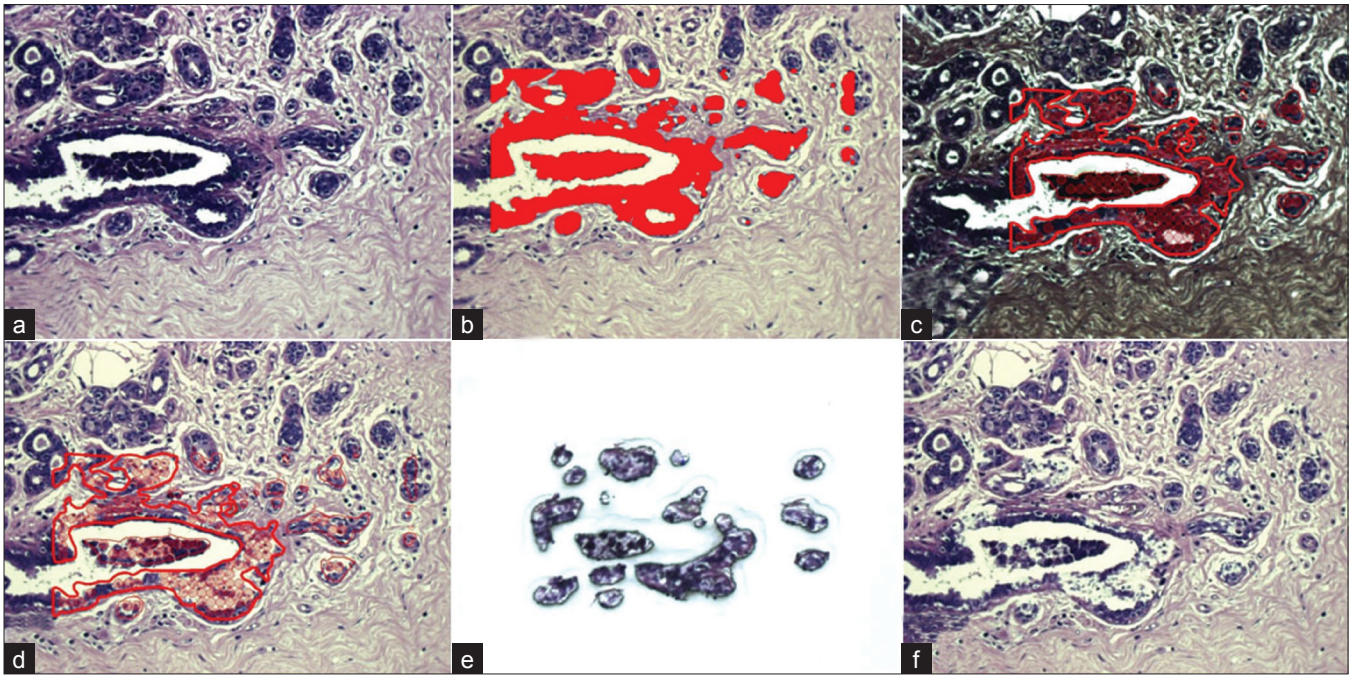

Figure 7: SIVQ–LCM of breast epithelium. (a) An FOV of HandE of FFPE normal breast tissue on a charged slide. A single vector was chosen to paint the epithelium (b). The paint was recognized by AutoScan, and a dissection map was created with laser shots autonomously fired within the map (c). The tissue was dissected and the remaining tissue and map are shown in (d). The microdissected cells are shown in (e). The remaining tissue is shown in (f)

with the samples obtained by conventional LCM alone, demonstrating the equivalency of the two dissection methods [Figure 6].

Microdissection at Different Length Scales

We were able to utilize SIVQ–LCM to dissect cells and structures at various length scales, using differently sized vectors; in other words, to use SIVQ to identify and threshold each of the following elements: overall histological field architecture, cellular phenotype, subcellular regions, cytoplasmic texture, and nuclear features. For the microdissection of normal esophageal epithelium

and tumor, the dissection was performed at 10× magnification [Figures 4 and 5, respectively]. For mid-range length scales of dissection, we used FFPE breast tissue on a standard glass slide and 20× magnification to dissect normal epithelium [Figure 7] and also to dissect a unique subset of the stroma [Figure 8]. The stromal SIVQ map was generated using a vector representing the unique stromal chrominance, luminance and textural data. The thresholded image was loaded into the Arcturus XT and the targeted region was then dissected. The quality of SIVQ–LCM stromal microdissection was improved in some cases by using membrane slides instead of glass, as shown in Supplemental Figure 1, where stroma from a dog prostate gland was dissected on a membrane slide.

At a smaller length scale (40× magnification), we microdissected single cells with a specific nuclear morphology from FFPE dog prostate tissue section. A vector was created to entirely encircle a particular size and textured nucleus with a prominent nucleoli and a glassy peri-nucleolar space [see vector image inset, Figure 9a]. This feature was queried against the entire field of view, including luminal, basal, and stromal cells. SIVQ identified this particular nuclear size and morphology in only 11 prostate luminal cells in the section and the painted image was loaded to the LCM instrument and then these 11 cells were auto-dissected [Figure 9]. The bottom-middle and bottom-right panels demonstrate the complete and specific microdissection of the cells consisting of their nuclei and corresponding luminal cytoplasm.

SIVQ analysis can also be applied to an immunohistochemically (IHC) stained slide and vectors created that recognize stained cells as well as cells with different labeling intensities [Figure 10a]. For example, in Figure 10b, we generated a vector to recognize only the dark brown chromogen (see vector insert image) and were able to selectively paint darkly stained areas. We then generated vectors to recognize lighter-staining [Figure 10c] and medium-staining cells [Figure 10d]. After SIVQ image painting, the image was transferred to the LCM instrument and the majority of IHC stained cells were dissected [Figure 10e], although a few cells remained on the slide [Figure 10f] since the section was placed on a charged glass slide (required for IHC) and this somewhat reduced the efficiency of LCM, which is not uncommon for standard immuno-LCM procedures.

DISCUSSION

Technical Challenges – Areas for Improvement

While many obstacles were overcome in the integration of SIVQ with LCM in this study, there are still aspects of the process that can be improved. SIVQ performs optimally with high-quality, high-resolution images, and the key limiting factor in this report, SIVQ–LCM work-flow, as presented in the work, is the generation of suitable quality images from a non–cover-slipped tissue section. The optimized staining protocol employed was sufficient for many SIVQ-based dissections; however, further improvements in image visualization are needed.

New stains could improve SIVQ–LCM. For example, the acidity of the keratins in squamous cell carcinoma of the esophagus caused an alteration of the coloring of Toluidine blue, thus allowing for contrast enhancement and successful microdissection. New yet-undefined stains may be beneficial for SIVQ-based microdissection of some cell types. Applying "digital" stains in a more elaborate way than the "Auto Correct" function used here could better enhance the image quality and cellular contrast to allow for more unique dissections. The methods we employed were sufficient for successful dissection; but these protocols likely represent only the beginning of the full potential discriminant power of SIVQ–LCM as applied to tissue slides, when fully developed.

Current LCM instruments write *x–y* coordinates into the microscopic images, allowing for multiple fields of view (FOVs) to be taken before microdissection. The integration of LCM with the expanded surface area represented by a typical WSI image would allow for more efficient and greater yield of biomolecules. Moreover, at present, images have to be exported from the LCM machine to the SIVQ discovery platform, and then back to the LCM machine, adding unnecessary work-flow complexity. With access to the application programming interface (API) of any contemporary LCM instrument, one could render the SIVQ morphologic gating function as a native component of the extant tissue capture process, allowing for "live" image analysis and enhanced throughput. Extrapolating to the likely revised WSI work-flow models of the not-too-distant future, where over 100 WSI slide scans would take place in an automated fashion, it would be possible to incorporate an SIVQ–LCM solution in that setting, enabling very high economies of scale for selective material capture.

Automation and Human Contact Time

Standard laser dissection requires tissue sections to be reviewed to histologically identify desired cells, requiring a pathologist or a scientist trained in histology before, during, and after microdissection. Thus, the rate-limiting step in high-throughput expression profiling is often the time required to identify and dissect an adequate number of cells. With the integration of SIVQ into LCM, expert observation is reduced by the semi-autonomous identification of target cells using a morphologic feature, whether it is architectural, cytologic, or nuclear. SIVQ–LCM can reduce the pathologist's role to selection of a new vector (or alternatively, choosing one from a future

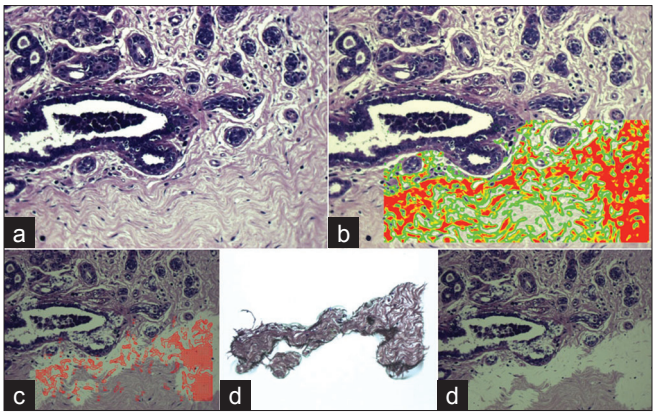

Figure 8: SIVQ–LCM of breast stroma. (a) An FOV of HandE of FFPE normal breast tissue on a charged slide. A single vector was chosen to paint the stroma (b). The paint was recognized by AutoScan, the cells were dissected and the remaining tissue and map are shown in (c). The microdissected cells are shown in (d). The remaining tissue is shown in (e)

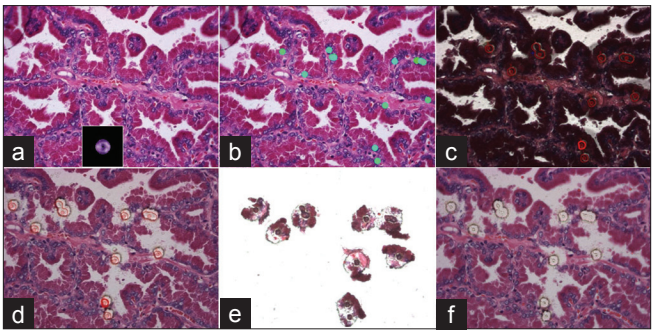

Figure 9: SIVQ–LCM of single cells. (a) An FOV of HandE of FFPE dog prostatic tissue on a membrane slide. A single vector was chosen (middle of figure) to identify single prostate luminal cells with prominent nucleoli and a glassy peri-nucleolar space (b). The paint was recognized by AutoScan, and a dissection map was created with laser shots that were manually placed within the map (c). The cells were dissected and the remaining tissue and map are shown in (d). The microdissected cells are shown in (e) where one can see 11 nuclei and their corresponding luminal cytoplasm. The remaining tissue is shown in (f)

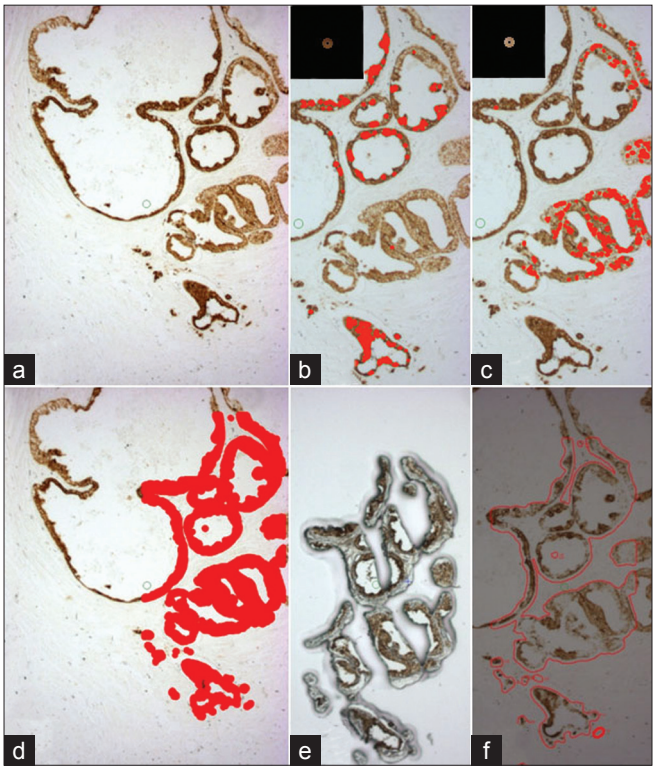

Figure 10: SIVQ-LCM of IHC stained tissue. (a) A cytokeratin IHC stain of prostatic tissue. A single vector (inset) was chosen to identify the dark brown chromagen (b). A single vector was chosen to identify the light brown chromagen (inset) (c). A single vector was chosen to paint all the brown chromagen in (d) and was then dissected as shown in (e), with the remaining tissue and dissection map shown in (f)

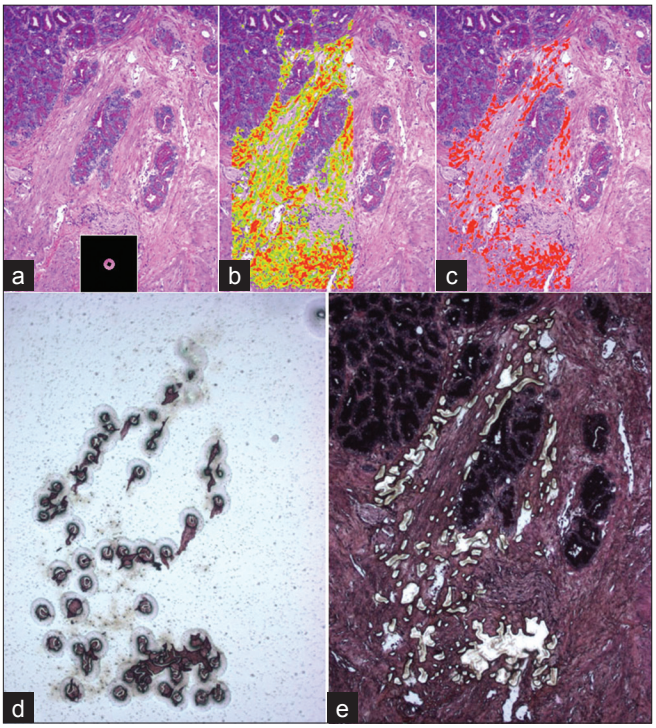

Supplemental Figure 1: SIVQ–LCM of dog prostatic stroma. (a) An FOV of HandE of FFPE normal dog prostatic tissue on a membrane slide. A single vector (shown above) was chosen to paint the epithelium (b). We were interested in only the stroma painted in red (c). The tissue was dissected and the procured cells are shown in (d) and the remaining tissue is shown in (e)

vector library) and then allowing for the subsequent steps to be carried out by technical personnel. The amount of time saved may appear minor when performing relatively limited dissections as described above. However, if the dissection requirement is several hundred thousand cells per case, multiplied by two or more cell populations per slide, and then multiplied by 25 cases, the time savings enabled by SIVQ–LCM grow by a very significant multiplier. With large, multi-institutional cohort studies, there likely will be an increasing requirement for such high-throughput tissue selection settings, where a significant quantity of tissue is required from a large cohort of identified study cases.

CONCLUSION

In the present study, we have demonstrated that the efficiency of LCM for capturing large numbers of cells quickly can be greatly improved by use of the recently described SIVQ feature matching algorithm. This algorithm was integrated in a turnkey fashion with a standard LCM workstation, making possible the creation of a high-throughput cell procurement instrument. Computer-aided LCM alters the work-flow of microdissection in several significant ways. First, it decreases the human–instrument contact time and allows for non-domain personnel to perform dissections on an equal caliber as SMEs. Second, the approach permits histologically constrained morphologies (e.g. automated selection of only the malignant epithelium of solid tissue tumors) to be acquired in a semi-autonomous fashion, allowing for the generation of large, preparative quantities of DNA, RNA, or protein for subsequent high-throughput analysis (e.g. as required for Next-Generation Sequencing or certain proteomic assays). Lastly, SIVQ–LCM holds unique potential as a discovery tool for molecular pathology, since individual cells with particular computer-defined morphologic features can be microdissected and profiled, thus creating a new generation of integrated and composite morphological data types (e.g. morpho-genomics or morpho-proteomics).

In summary, SIVQ–LCM is a new technical duo that facilitates automated, large-scale interrogation of unique and defined highly precise cell populations.

ACKNOWLEDGMENTS

The study was supported in part by the Center for Cancer Research in the intramural program of the National Cancer Institute, NIH, and at the University of Michigan by Clinical Translational Science Award (CTSA) 5ULRR02498603 PI Ken Pienta, and in part by 5U54GM062119-10 entitled Inflammation and the Host Response to Injury, a Large-Scale Collaborative Research Program funded by NIGMS. We would like to acknowledge Dr. Mehmet Toner and Dr. Ronald Tomkins from Massachusetts General Hospital, Harvard Medical School, for their continued assistance with the development and use of core functionality of the SIVQ algorithm.

REFERENCES

1. Emmert-Buck MR, Bonner RF, Smith PD, Chuaqui RF, Zhuang Z, Goldstein SR, *et al*. lLaser capture microdissection. Science 1996;274:998-1001.
2. Espina V, Wulfkuhle JD, Calvert VS, VanMeter A, Zhou W, Coukos G, *et al*. Laser-capture microdissection. Nat Protoc 2006;1:586-603.
3. Hunt JL, Finkelstein SD. Microdissection techniques for molecular testing in surgical pathology. Arch Pathol Lab Med 2004;128:1372-8.
4. Harrell JC, Dye WW, Harvell DM, Sartorius CA, Horwitz KB. Contaminating cells alter gene signatures in whole organ versus laser capture microdissected tumors: A comparison of experimental breast cancers and their lymph node metastases. Clin Exp Metastasis 2008;25:81-8.
5. El-Serag HB, Nurgalieva ZZ, Mistretta TA, Finegold MJ, Souza R, Hilsenbeck S, *et al*. Gene expression in Barrett's esophagus: laser capture versus whole tissue. Scand J Gastroenterol 2009;44:787-95.
6. Klee EW, Erdogan S, Tillmans L, Kosari F, Sun Z, Wigle DA, *et al*. Impact of sample acquisition and linear amplification on gene expression profiling of lung adenocarcinoma: Laser capture micro-dissection cell-sampling versus bulk tissue-sampling. BMC Med Genomics 2009;2:13.
7. Silvestri A, Colombatti A, Calvert VS, Deng J, Mammano E, Belluco C, *et al*. Protein pathway biomarker analysis of human cancer reveals requirement for upfront cellular-enrichment processing. Lab Invest 2010;90:787-96.
8. Tangrea MA, Chuaqui RF, Gillespie JW, Ahram M, Gannot G, Wallis BS, *et al*. Expression microdissection: Operator-independent retrieval of cells for molecular profiling. Diagn Mol Pathol 2004;13:207-12.
9. Hanson JC, Tangrea MA, Kim S, Armani MD, Pohida TJ, Bonner RF, *et al*. Expression Microdissection (xMD) Adapted to Commercial Laser Dissection Instruments Nature Protocols 2010 [In Press].
10. Hipp JD, Cheng J, Mehmet T, Tomkins R, Balis U. Spatially Invariant Vector Quantization: A pattern matching algorithm for multiple classes of image subject matter- including Pathology. J Pathol Inform 2011, 2:13.
11. Erickson HS, Albert PS, Gillespie JW, Rodriguez-Canales J, Marston Linehan W, Pinto PA, *et al*. Quantitative RT-PCR gene expression analysis of laser microdissected tissue samples. Nat Protoc 2009;4:902-22.